



NRC Publications Archive Archives des publications du CNRC

Supported lipid bilayers on biocompatible polysaccharide multilayers Mulligan, Kirk; Jakubek, Zygmunt J.; Johnston, Linda J.

This publication could be one of several versions: author's original, accepted manuscript or the publisher's version. / La version de cette publication peut être l'une des suivantes : la version prépublication de l'auteur, la version acceptée du manuscrit ou la version de l'éditeur.

For the publisher's version, please access the DOI link below. / Pour consulter la version de l'éditeur, utilisez le lien DOI ci-dessous.

Publisher's version / Version de l'éditeur:

<https://doi.org/10.1021/la203207p>

Langmuir, 27, 23, pp. 14352-14359, 2011-10-20

NRC Publications Record / Notice d'Archives des publications de CNRC:

<https://nrc-publications.canada.ca/eng/view/object/?id=9c3c6cd6-bdf5-4d3b-a046-ee0f0eeb09b0>

<https://publications-cnrc.canada.ca/fra/voir/objet/?id=9c3c6cd6-bdf5-4d3b-a046-ee0f0eeb09b0>

Access and use of this website and the material on it are subject to the Terms and Conditions set forth at

<https://nrc-publications.canada.ca/eng/copyright>

READ THESE TERMS AND CONDITIONS CAREFULLY BEFORE USING THIS WEBSITE.

L'accès à ce site Web et l'utilisation de son contenu sont assujettis aux conditions présentées dans le site

<https://publications-cnrc.canada.ca/fra/droits>

LISEZ CES CONDITIONS ATTENTIVEMENT AVANT D'UTILISER CE SITE WEB.

Questions? Contact the NRC Publications Archive team at

PublicationsArchive-ArchivesPublications@nrc-cnrc.gc.ca. If you wish to email the authors directly, please see the first page of the publication for their contact information.

Vous avez des questions? Nous pouvons vous aider. Pour communiquer directement avec un auteur, consultez la première page de la revue dans laquelle son article a été publié afin de trouver ses coordonnées. Si vous n'arrivez pas à les repérer, communiquez avec nous à PublicationsArchive-ArchivesPublications@nrc-cnrc.gc.ca.



Supported Lipid Bilayers on Biocompatible Polysaccharide Multilayers

Kirk Mulligan^{1,2}, Zygmunt J. Jakubek¹ and Linda J. Johnston^{1,2}

¹Steacie Institute for Molecular Sciences, National Research Council of Canada

100 Sussex Drive, Ottawa, ON, Canada K1A 0R6

and

²Department of Chemistry, University of Ottawa

Ottawa, ON, Canada K1N 6N5

Abstract

The formation of supported lipid bilayers on soft polymer cushions is a useful approach to decouple the membrane from the substrate for applications involving membrane proteins. We have prepared biocompatible polymer cushions by the layer-by-layer assembly of two polysaccharide polyelectrolytes, chitosan (CHI) and hyaluronic acid, on glass and silicon substrates. (CHI/HA)₅ films were characterized by atomic force microscopy, giving an average thickness of 57 and roughness of 25 nm in aqueous solution at pH 6.5. Formation of zwitterionic lipid bilayers by the vesicle fusion method was attempted using DOPC vesicles at pH 4 and pH 6.5 on (CHI/HA)₅ films. At higher pH adsorbed lipids had low mobility and large immobile lipid fractions; a combination of fluorescence and AFM indicated that this was attributable to the formation of poor quality membranes with defects and pinned lipids, rather than to a layer of surface adsorbed vesicles. By contrast, more uniform bilayers with mobile lipids were produced at pH 4. Fluorescence recovery after photobleaching gave diffusion coefficients that were similar to those for bilayers on PEG cushions and considerably higher than those measured on other polyelectrolyte films. The results suggest that the polymer surface charge is more important than the surface roughness in controlling the formation of mobile supported bilayers. These results demonstrate that polysaccharides provide a useful alternative to other polymer cushions, particularly for applications where biocompatibility is important.

INTRODUCTION

Solid-supported phospholipid bilayers are widely used as models to understand the function of cellular membranes and as platforms for membrane protein biosensing applications based on electrical or optical detection.¹⁻³ Supported lipid bilayers have a number of advantages over other types of model membranes: they are stable and can be easily prepared over large surface areas, there is a thin layer of water (<2 nm) between the support and the lower leaflet of the membrane, which leads to lipid mobilities that are similar to those in vesicles and they can be characterized by a range of surface-specific analytical techniques. Nevertheless, the proximity of the membrane to the solid support is a major limitation for applications that involve incorporation of integral membrane proteins. Many proteins have large domains that protrude from the membrane by several nanometers and cannot be easily accommodated in the thin water layer that separates the lower leaflet of the supported bilayer from the surface. Interactions with the underlying solid surface interfere with both the lateral mobility and function of the protein.

Several approaches have been employed to decouple the supported bilayer from the underlying support. One method utilizes modified lipids in which the head groups have long chain tethers that can be covalently attached to the underlying surface, thus providing space under the bilayer to accommodate bulky membrane domains.⁴⁻⁶ Tethers are usually attached to the surface using either silane or gold-thiol chemistry. A second and more widely used approach is to construct lipid bilayers on soft polymer cushions.^{1,7,8} In some cases bilayers are constructed directly on top of thin layers of surface adsorbed polymers, such as cellulose, or a surface grafted polymer.^{9,10} Another method involves the use of polymer spacers which have one end attached to lipid head groups and the other end functionalized for surface attachment using either radical or silane chemistry.^{11,12} This method provides flexibility to modify the thickness and viscosity of the polymer layer, but requires a multi-step fabrication process with the initial construction of the polymer layer and lower membrane leaflet by Langmuir-Blodgett transfer of a monolayer containing the polymer-modified lipid; this is followed by addition of the upper bilayer leaflet by either vesicle fusion or Langmuir-Schaeffer transfer of a second lipid monolayer and finally treatment to covalently attach the polymer layer to the surface. Several recent studies have shown that covalent attachment of the polymer to the surface is not essential, somewhat simplifying the procedure.¹³⁻¹⁶ Nevertheless, the requirement for lipid-

polymer conjugates, and the complex assembly (relative to vesicle fusion methods) are limitations for eventual scale-up and/or multiplexing for biosensing applications.

Polyelectrolyte multilayers (PEMs) provide an interesting alternative to other types of polymer cushions. They are constructed by alternating adsorption of positively and negatively charged polyelectrolytes to a charged surface, usually by the layer-by-layer deposition technique.^{17,18} The assembly of PEM films is governed primarily by electrostatic interactions and their properties (thickness, roughness, surface charge) can be controlled by varying the number of adsorption cycles, the molecular weight, charge density and concentration of the polyelectrolytes, and the ionic strength and pH of the solutions. Several studies have shown that stable supported lipid bilayers can be formed on PEMs composed of alternating layers of polystyrenesulfonate (PSS) and poly-(allylamine hydrochloride) (PAH).¹⁹⁻²¹ Charged polysaccharides are also well-known to form PEMs by the layer-by-layer assembly method.^{22,23} The biocompatibility, ready availability and low cost of charged polysaccharides have made them attractive choices for a range of applications, including drug delivery vehicles based on lipid-polyelectrolyte particles, biocompatible surfaces for controlling cell growth and tissue biomimetics.²³⁻²⁸

We have examined the suitability of PEM films constructed from alternating layers of chitosan (CHI) and hyaluronic acid (HA) as polymer cushions for supported lipid bilayers. Although polysaccharide-lipid interactions have been exploited for drug delivery applications, to the best of our knowledge polysaccharide PEMs have not been used as supports for lipid bilayers. Hyaluronic acid is an anionic linear polysaccharide (pKa ~3.0) with a repeating disaccharide structure consisting of 2-acetamide-2-deoxy- β -D-glucose and β -D-glucuronic acid residues.²⁹ HA is found in the extracellular matrix of all higher animals and has been shown to affect cellular functions such as migration, adhesion, and proliferation. Chitosan is a random copolymer of N-acetyl- β -D-glycosamine and β -D-glycosamine that is obtained by deacetylation of chitin and has a pKa of ~6.5.³⁰ CHI/HA PEMs were prepared and characterized by atomic force microscopy (AFM) and ellipsometry and used as substrates for preparation of supported DOPC bilayers by vesicle fusion. Bilayers were characterized by a combination of AFM, fluorescence microscopy and fluorescence recovery after photobleaching (FRAP). The results show that the formation of bilayers with mobile lipids is dependent on the pH used for bilayer preparation. At pH 6.5 heterogeneous bilayers with slowly diffusing lipids

and large immobile fractions are formed; we conclude that a combination of the surface roughness of the underlying polymer and pinning of individual lipids may contribute to the complex behavior. By contrast, uniform bilayers with diffusion coefficients that are similar to bilayers on glass and other polymer supports are obtained at pH 4, indicating the utility of polysaccharide PEMs for preparation of supported lipid bilayers.

MATERIALS AND METHODS

Materials. Lipids (1,2-dioleoyl-sn-glycero-3-phosphocholine (DOPC), egg sphingomyelin and cholesterol) and 1,2-dipalmitoyl-sn-glycero-3-phosphoethanolamine-N-[methoxy(polyethylene glycol)-2000] (PEG-DPPE) were obtained from Avanti Polar Lipids and were used as received. All aqueous solutions were prepared with 18.3 M Ω cm Milli-Q water. Texas Red 543 1,2-dihexadecanoyl-sn-glycero-3-phosphoethanolamine (TR-DHPE) and Oregon Green 488 1,2-dihexadecanoyl-sn-glycero-3-phosphoethanolamine (OG-DHPE) were obtained from Invitrogen. Low molecular weight chitosan (CHI, MW = 5 x 10⁴ g/mol), hyaluronic acid sodium salt (HA, MW = 1.63 x 10⁶ g/mol) from *Streptococcus equi* and all other materials were obtained from Aldrich (\geq 98% pure) and used as received. Branched poly(ethyleneimine), MW 1800, 99% was obtained from Polysciences, Inc. Cobalt(II) chloride hexahydrate was from Riedel-deHaen. Glass coverslips (No. 1, 25 mm) from Fisher Scientific and n-type silicon (111) wafers polished on one side with a thickness of 250 \pm 25 μ m and a resistance of 1.0-5.0 ohm \cdot cm were used for preparation of PEMs.

Assembly of PEM. The polyelectrolyte multilayers were constructed following the previously described layer-by-layer assembly method on either glass or silicon substrates.^{22,31} Substrates were cleaned prior to use by dipping in a piranha solution consisting of 70% concentrated sulfuric acid and 30% hydrogen peroxide, followed by rinsing with Milli-Q water, and nitrogen drying. Polyelectrolyte solutions (1.0 g L⁻¹) were prepared in 0.15 M NaCl and the pH was adjusted to 4.5 using aqueous concentrated acetic acid solution. Polymer solutions were filtered through a 0.45 μ m Millipore PVDF filter prior to use. The cleaned substrate was placed in a homemade glass fluid cell holder. The cell was immersed in aqueous CHI solution for 15 min and then removed and placed in a beaker containing 350 mL of NaCl solution (0.15 M, pH 4.5) for 1 min. The cell was then removed and placed in a second beaker containing 150 mL of NaCl solution (0.15 M, pH 4.5) for another 5 min to ensure the removal

of excess CHI. HA was then deposited on the substrate surface following the dipping/rinsing procedure described above for CHI. The assembly of the PEM was continued up to 5 bilayers. Rinsing beakers containing aqueous NaCl solution were changed after 3 uses. The PEM coated substrates were dried by a stream of N₂ and stored in a nitrogen box until used for bilayer preparation, typically within 1-2 days and never more than 1 week.

Preparation of Small Unilamellar Vesicles. Chloroform solutions of lipids were mixed in the appropriate ratios, the solvent was removed, and the film was dried under vacuum overnight. The lipid films were then hydrated in Milli-Q water containing (a) 10 mM CaCl₂ and 140 mM NaCl at the desired pH, 4 or 7 (for preparation of PEM-supported bilayers) or (b) 10 mM NaH₂PO₄ and 100 mM KCl (for preparation of PEG-supported bilayers) and vortexed to obtain multilamellar vesicles. Small unilamellar vesicles were prepared by bath sonication with an initial temperature of 20°C to form clear dispersions with a final lipid concentration of 1 mg/mL. Vesicles prepared by bath sonication were typically ~40 nm in diameter, as assessed by dynamic light scattering. Vesicles were stored at 4°C and used within 1 week.

Preparation of Supported Bilayers. (a) PEMs: An aliquot of vesicle solution (100 μL) and Milli-Q water (400 μL) containing 10 mM CaCl₂ and 140 mM NaCl at the desired pH, 4 or 7, were added to a (CHI/HA)₅ PEM substrate and clamped into a TIRF or AFM liquid cell. After incubation at room temperature overnight, the bilayers were rinsed extensively with Milli-Q water containing 140 mM NaCl at the corresponding pH to remove unattached vesicles before imaging. (b) PEG polymers: A polymer-doped monolayer was prepared by Langmuir-Blodgett deposition on a Nima 611 trough. A 1 mg/mL solution of DOPC with 7 mol% PEG-DPPE was prepared in chloroform and 20 μL of the lipid solution was deposited at the air-water interface. After waiting 15 minutes to allow for chloroform evaporation, the lipids were compressed to a surface pressure of 32 mN/m. Two glass coverslips placed back to back were then raised vertically out of the trough at a rate of 15 mm/min, allowing the deposition of a PEG-supported lipid monolayer on only the exposed side of each coverslip. An aliquot of vesicle solution (100 μL) and Milli-Q water (300 μL) containing 10 mM NaH₂PO₄ and 100 mM KCl, were added to the monolayer-coated substrate and clamped into a TIRF or AFM liquid cell. After incubation at room temperature for 1h, the bilayers were rinsed extensively with Milli-Q water containing 10 mM NaH₂PO₄ and 100 mM KCl to remove unattached vesicles before imaging.

Atomic Force Microscopy. The AFM images were obtained at room temperature ($22\pm 1^\circ\text{C}$) using a PicoSPM atomic force microscope (Molecular Imaging) in MAC-mode. Magnetic coated silicon tips with spring constants of ~ 0.5 N/m and resonance frequencies between 5 and 40 kHz in aqueous solution were used. A $30 \times 30 \mu\text{m}^2$ scanner was operated at a scan rate between 0.7 and 1.3 Hz. The images shown are flattened raw data. Two or more independently prepared samples were imaged for each set of conditions with several areas scanned for each sample. Reported PEM thicknesses are based on the removal of polymer with a razor blade and measuring the AFM step height for at least two independent samples with a minimum of nine areas imaged.

Fluorescence Microscopy. Fluorescence images of bilayers were taken on an Olympus IX81 total internal reflection fluorescence (TIRF) microscope equipped with a back-illuminated electron multiplying CCD camera (Cascade 512B, Photometrics) and a $60\times/1.45$ NA Plan Achromat TIRF objective (Olympus). Supported bilayers containing either Texas Red DHPE or Oregon Green DHPE (0.2 mol%) were excited at 543 or 488 nm, respectively. A 150x objective was used for several experiments (pixel size – 107×107 nm, compared to 267×267 nm for the 60x objective). Images shown are all measured in TIRF mode, although comparison of TIRF and epifluorescence images gave very similar results except for reduced interference from adsorbed vesicles in the TIRF images.

Fluorescence Recovery After Photobleaching (FRAP). FRAP experiments for bilayers labeled with 0.2 % Oregon Green DHPE were conducted on an Olympus IX81 microscope (epifluorescence mode) by bleaching a $\sim 45 \mu\text{m}$ diameter spot with full laser power (~ 11 mW) at 488 nm for 1-3 s. The fluorescence recovery was recorded with a 150x objective with a 1-5 second interval (depending on the recovery kinetics) between images at a reduced laser power (< 2.3 mW). Image analysis was performed using National Institutes of Health Image J software (<http://rsb.info.nih.gov/ij/>). Diffusion coefficients were estimated following the approach of Soumpasis with normalized intensities fit to a two-dimensional diffusion equation.³² Reported diffusion coefficients and mobile fractions are the average of bleaching experiments on multiple areas for at least 2 independently prepared bilayers.

Ellipsometry. Thickness measurements of dry PEM coated silicon substrates were estimated using a Gaertner model L116S single wavelength (633 nm) ellipsometer at an angle of incidence of 70° . A two-layer model with $n=1.46$ as the refractive index of the PEM layer

and the silicon substrate described by $n=3.85$ and $k=0.02$ was used to estimate the PEM dry thickness.

RESULTS AND DISCUSSION

Preparation and Characterization of CHI/HA Films. The assembly of PEM films composed of alternating layers of HA and CHI has been examined in considerable detail by several groups.^{22,23,25,31,33,34} Based on the literature data we selected films consisting of 5 bilayers, starting with adsorption of CHI to either glass or silicon surfaces; this selection provided a reasonable compromise between having a polymer film of sufficient thickness to provide good surface coverage while minimizing the surface roughness, which tends to increase with film thickness. We also reasoned that the use of a negatively charged top HA layer would be the most suitable for forming bilayers of zwitterionic lipids based on the rapid formation of bilayers by vesicle fusion on hydrophilic, negatively charged surfaces such as mica and glass.³⁵ AFM images of a (CHI/HA)₅ film on a glass substrate imaged in water (pH 6.5) are shown in Figure 1A, B. The film surface is covered with densely packed, round or slightly elliptical features that range in height from ~20 nm to ~150 nm, with typical widths of several hundred nanometers. The film thickness was assessed by scratching away part of the film to expose the bare substrate and measuring the step height by AFM, as shown in a representative image in Figure 1C. The average thickness and rms roughness of the (CHI/HA)₅ polymer film were found to be 57 ± 3 nm and 25 ± 2 nm, respectively, Table 1. For comparison, films were also prepared by sequential addition of 5 CHI/HA bilayers to glass coated with a poly(ethyleneimine) (PEI)/HA bilayer; similar film morphology, thickness and surface roughness were measured, indicating that there was no particular advantage to the presence of the initial PEI surface layer. Since bilayer formation was attempted at several pHs, the (CHI/HA)₅ film thickness and roughness were also measured at pH 4; a reduced film thickness and roughness of 31 ± 4 nm and 15 ± 3 nm were obtained. Previous studies have shown that HA/CHI films are stable in contact with aqueous solutions with pH between 3.5 and 9, and show modest changes in thickness over this range.³³ The films are not stable in more basic or more acidic solutions, since neutralization of one of the polyelectrolytes leads to a charge imbalance that destroys the film.³³

For comparison, (CHI/HA)₅ polymer films were prepared on a silicon (111) substrate. The representative AFM image shown in Figure 1D indicates a similar film morphology to that obtained on glass, although the raised features were more elongated and interconnected. The thickness and rms roughness of the (CHI/HA)₅ polymer film were found to be 52±5 nm and 23±2 nm, respectively. Ellipsometry was used to measure an average thickness of 32±4 nm for a dry (CHI/HA)₅ film on silicon (111).

The film thickness and morphology are analogous to those reported in the literature for CHI/HA films prepared under similar conditions. For example, Picart and coworkers obtained films with comparable structures as assessed by AFM for (CHI/HA)_n films, although neither film thickness nor roughness was reported for a sample with n = 5 bilayers.²³ Winnik and coworkers prepared films with similar morphologies on a PEI-coated thiol monolayer formed by self-assembly on a gold surface; for PEI-(HA/CHI)₅ films they report surface thickness and roughness of 70 nm and 20 nm, respectively.³¹ These results are in good agreement with those obtained here considering the differences in the substrate and the molecular weight of the polyelectrolytes and the opposite charge for the top polyelectrolyte layer in the two cases. Previous studies have shown that PEM film formation occurs by initial formation of small individual islands that grow in size and eventually coalesce as additional polyelectrolyte is adsorbed on or between them.²³ The slight change in film morphology observed for films on glass and silicon indicates that for our experimental conditions the adsorption of 5 bilayers is close to the transition between growing islands and interconnected structures.

Formation of DOPC Bilayers on (CHI/HA)₅ Films. In initial attempts to form supported bilayers on (CHI/HA)₅ films, DOPC vesicles containing 0.2 mol % TR-DHPE were incubated with polymer-coated glass in water in the presence of 10 mM CaCl₂ and 140 mM NaCl overnight at pH 6.5, followed by extensive washing to remove adsorbed vesicles. Fluorescence microscopy was used to assess the quality of the adsorbed lipid sample. As shown in Figure 2A, the samples showed patchy fluorescence with occasional small dark areas and bright features that are assigned to defects and adsorbed vesicles, respectively. For comparison a TR-DHPE-labeled DOPC bilayer on glass is shown in Figure 2B; the DOPC bilayer on glass is significantly more uniform than the membrane obtained on the PEM film. In order to test for lipid mobility a FRAP experiment was attempted for a bilayer labeled with

0.2 mol % OG-DHPE on a (CHI/HA)₅ film (Figure 2C). Images before and after photobleaching are shown in Figure 3, along with a plot demonstrating a large immobile lipid fraction. Replicate experiments on several samples indicated that the mobile lipid fraction was typically between 10-30%, with diffusion coefficients, *D*, that varied between 0.1 and 0.5 μm²/s. For comparison, FRAP experiments for OG-DHPE in DOPC bilayers prepared by vesicle fusion on glass gave a diffusion coefficient of 4.4 μm²/s (Table 2) with a mobile fraction of ~100%. Literature values for *D* for fluid-phase supported lipid bilayers on either glass or mica are in the range of 1-6 μm²/s, depending on the lipid, substrate and presence of salt and buffer.^{36,37}

The low diffusion coefficients, large fraction of immobile lipids and variable results for individual samples could indicate a significant fraction of surface adsorbed vesicles that have not ruptured and fused to give a supported membrane. Alternately, this observation may reflect the formation of a heterogeneous bilayer with many small defects and/or with lipids pinned to the underlying polymer. In order to distinguish between these possibilities, a similar sample was imaged by AFM, Figure 4. The images show an uneven surface that reflects the roughness of the initial polymer surface. However, the measured roughness of 17±3 nm is significantly smaller than that for the initial hydrated PEM film (>50 nm), and the surface morphology shows no evidence for the presence of a layer of surface-adsorbed vesicles. The combined results from the fluorescence imaging, FRAP and AFM analysis suggest that incubation of DOPC vesicles with (CHI/HA)₅ films at pH 6.5 gives a surface adsorbed bilayer with a large fraction of immobile lipids, either due to numerous defects, the presence of a rough polymer surface or lipid pinning to the PEM film. Note that the surface roughness makes it impossible to detect small membrane defects that would normally be observable by AFM.

An additional fluorescence quenching experiment was carried out to probe whether differences in the distribution of dye between the two bilayer leaflets contributed to the variable results for lipid mobility and mobile fraction. Cobalt ions have been shown not to penetrate lipid bilayers at concentrations below 100 mM³⁸ and are thus compatible with selectively quenching fluorophores in the top leaflet of a supported bilayer.³⁹ Fluorescence images were measured for a DOPC bilayer on a (CHI/HA)₅ film at pH 6.5 before and after addition of 50 mM CoCl₂. The total intensity decreased by 50 ± 5 % (average of two

experiments) after adding Co^{2+} , indicating that approximately half of the dye was accessible to the quencher, presumably due to its location in the top leaflet of the bilayer. A FRAP experiment for a bilayer at pH 6.5 before Co^{2+} addition gave $D = 0.5 \mu\text{m}^2/\text{s}$, with a mobile fraction of 44%; a FRAP experiment for the same bilayer after the addition of Co^{2+} showed no recovery of photobleaching over the same time period, indicating $D < 0.05 \mu\text{m}^2/\text{s}$. These experiments indicate that pinning of lipids in the lower bilayer leaflet is a major contributor to the slow diffusion and low mobile fractions for DOPC bilayers on PEM films.

The formation of lipid bilayers by vesicle fusion is very sensitive to the surface properties, including charge, with surfaces such as glass, mica or silicon being the most widely used.³⁵ A recent study has shown that adjusting the surface charge by varying pH is a useful approach to promote formation of a homogeneous bilayer on a surface grafted film of maleic acid copolymers; in this case variation of the pH was used to minimize electrostatic repulsion between vesicles with 20% negatively charged lipids and the negatively charged polymer layer.⁹ Similarly, systematic variation of the surface charge density using functionalized alkanethiol self-assembled monolayers demonstrated that there is an optimal charge density for formation of supported bilayers from PC vesicles.⁴⁰ Although neither of these examples is identical to the current system of charged polyelectrolytes, we tested the impact of varying the pH within the range of stable CHI-HA films on the quality of the bilayers. TIRF images for a $(\text{CHI}/\text{HA})_5$ film incubated with DOPC vesicles (labeled with either TR-DHPE, A or OG-DHPE, B) at pH 4 are shown in Figure 5. The bilayers are slightly more homogeneous than those formed at pH 6.5, although occasional defects and adsorbed vesicles are still visible. However, in this case the lipid mobility was considerably higher, as assessed by FRAP experiments. A representative experiment is shown in Figure 6, demonstrating complete recovery of the bleached area, with $D = 2.5 \mu\text{m}^2/\text{s}$, Table 2. The measured diffusion coefficient is approximately half that measured for DOPC on glass, indicating relatively minor effects of the PEM support on lipid diffusion. The surface roughness may partially account for the lower apparent diffusion coefficient since the actual surface area covered by the bilayer is larger than the area of the bleached spot.

DOPC bilayers at pH 4 showed similar quenching behavior to those at higher pH, with 46% quenching of the initial intensity after addition of 50 mM Co^{2+} . However, FRAP experiments before and after Co^{2+} addition did not show the large difference that was observed

at pH 6.5. FRAP for a DOPC bilayer before Co^{2+} addition gave $D = 2.8 \mu\text{m}^2/\text{s}$ with 98% mobile fraction. After Co^{2+} addition FRAP measurements of the same bilayer gave $D = 1.9 \mu\text{m}^2/\text{s}$ with 98% mobile fraction, indicating only a modest reduction in mobility for lipids in the lower leaflet.

To confirm that bilayers containing gel phase lipids could also be formed on PEM films, we tested a ternary lipid mixture that forms phase separated liquid-ordered domains surrounded by a fluid phase.^{41,42} Fluorescence images of samples obtained after incubating DOPC/egg sphingomyelin/cholesterol (2:2:1 molar ratio, 0.2 % TR-DHPE) vesicles with PEM films were similar to those obtained for DOPC vesicles, with no evidence for formation of dark domains that exclude the dye (data not shown). Both samples were also imaged using a higher magnification objective (150x, Figure 5C, D). There are slight differences between the two suggesting that small domains may be present for the ternary lipid mixture, although they are considerably smaller than those typically observed for bilayers on mica substrates.⁴¹ This is consistent with the observation that heating the sample above the melting transition temperature during bilayer formation produces domains that are larger than those obtained at room temperature.⁴¹

In order for PEMs to be generally useful as biocompatible supports for protein-containing bilayers, it may be necessary to work at closer to neutral pH. Therefore we tested the lipid mobility for DOPC bilayers that were formed by incubation at pH 4, and then rinsed with aqueous NaCl solution at pH 7. FRAP data gave a diffusion coefficient, $D = 2.8 \mu\text{m}^2/\text{s}$ (Table 2), similar to that obtained at pH 4, indicating that the pH can be readjusted after bilayer formation without reducing lipid mobility. The latter may be an important consideration for applications involving membrane proteins. The effect of pH on a membrane formed at pH 6.5 was also tested. A FRAP experiment for an initial bilayer at pH 6.5 gave $D = 0.2 \mu\text{m}^2/\text{s}$ with 16% mobile fraction. The bilayer was then washed with pH 4 solution and stored overnight at this pH prior to a second FRAP experiment which gave $D = 0.5 \mu\text{m}^2/\text{s}$ and a mobile fraction of 32%. This indicates that equilibration of the supported bilayer at low pH leads to somewhat higher mobile fraction and diffusion coefficient, presumably due to equilibration of the sample and repair of defects. However, the bilayer quality as assessed by lipid diffusion is still significantly better when the supported bilayer is formed at pH 4. It should also be noted that the pH of the lower bilayer leaflet may not have equilibrated to the value of the bulk solution.

Comparison to other polymer supported bilayers. Several recent reports have characterized supported lipid bilayers on polyethylene glycol (PEG) cushions.^{11,12,14,15} For comparison, a PEG-supported bilayer was prepared by the following procedure. First a DOPC monolayer with 7% PEG-DPPE was prepared at the air water interface and transferred to a glass slide; the polymer concentration is in the brush regime, slightly past the crossover point where the PEG chains are in contact with each other.¹⁴ The second bilayer leaflet was then constructed by fusion of DOPC vesicles containing 0.2% OG-DHPE. FRAP gave a measured diffusion coefficient of $2.16 \mu\text{m}^2/\text{s}$, slightly lower than D for DOPC bilayers on CHI/HA PEMs. This measurement is in good agreement with the D values of $1.5 \mu\text{m}^2/\text{s}$ and $2.3\text{-}2.7 \mu\text{m}^2/\text{s}$ for diffusion of NBD-PE in DPhPC and POPC bilayers prepared by vesicle fusion to a PEG-containing monolayer^{14,43} and with D values of $\sim 1.8 \mu\text{m}^2/\text{s}$ for a SOPC bilayer supported on a physisorbed lipopolymer, dioctadecylamine [poly(ethyloxazoline)].¹⁶ Similarly, D values of $1\text{-}2.5 \mu\text{m}^2/\text{s}$ with mobile fractions $>70\%$ have been reported for fluid PC bilayers on PEG cushions grafted to a glass surface.¹¹ In addition to these results using LB-LS or LB-vesicle fusion methods, vesicle fusion of POPC vesicles doped with low mol fractions of PEG-PE can also be used to produce PEG cushioned-bilayers. However, this method may not be of general utility due to the presence of polymer attached to the upper leaflet of the bilayers, thus reducing the accessibility for binding for biosensing applications.⁴⁴

A recent detailed study by Fischlechner and coworkers employed a combination of fluorescence, lipid adsorption measurements using a quartz crystal microbalance and infrared spectroscopy to investigate the adsorption of POPC/POPS vesicles on PSS/PAH PEMs.²¹ FRAP measurements indicated that the best quality bilayer ($D = 0.38 \mu\text{m}^2/\text{s}$) was formed from equimolar mixtures of POPC/POPS on PEMs with a positively charged PAH top layer.²¹ POPC vesicles adsorbed strongly to PEM films with either PAH or PSS as the top layer but did not rupture and spread to give a continuous bilayer, resulting in negligible lipid diffusion ($D \sim 0.001 \mu\text{m}^2/\text{s}$ for PAH). Although POPS vesicles did rupture on the surface to give bilayer patches, the strong binding of lipid to PAH amino groups as assessed by IR studies resulted in patchy and immobile bilayers. These results led to the conclusion that the ability to form mobile bilayers on the PSS/PAH films involves a subtle balance between the long range electrostatic interactions that are necessary for vesicle adsorption, spreading and rupture and the lipid mobility required for formation of a continuous bilayer. A related NMR and

fluorescence study concluded that a “somewhat” continuous POPC/POPS bilayer was formed on a PAH(PSS/PAH)₃ PEM, since there was evidence for small defects that allowed access of ions to both leaflets of the bilayer.¹⁹

Our results indicate that it is possible to form mobile zwitterionic bilayers on polysaccharide PEMs with negatively-charged HA in the top layer at pH 4, by contrast to the results for PSS/PAH films. The polysaccharide PEM cushions therefore provide a useful alternative to other polymer films for preparation of supported bilayers. The polysaccharides are biocompatible and the layer-by-layer assembly fabrication of PEM films is straightforward to use and does not require chemical modification of the surface. Bilayers on CHI/HA films have lipid mobilities that are comparable to those on various PEG polymer cushions and only slightly lower than those on glass. Our results show that the bilayer quality is poor when membrane formation is carried out at close to neutral pH and that there is a large difference in lipid mobility between the two leaflets. However, homogeneous bilayers formed at pH 4 retain their high lipid mobility in neutral solutions. These results are analogous to an earlier report showing that a low density of surface-adsorbed vesicles on anionic maleic acid copolymer films at pH 7 impedes bilayer formation for vesicles containing 20% negatively charged lipids; by contrast, lowering the pH reduces the electrostatic repulsion between the polymer film and vesicles, allowing the adsorption of a higher vesicle concentration and formation of a supported bilayer.⁹ The same study found that a strong correlation between lipid mobility and surface hydrophilicity with a measured diffusion coefficient of 1.2 $\mu\text{m}^2/\text{s}$ for the most hydrophilic surface and a five-fold reduction for the most hydrophobic. In the present study we find that a reduction in surface charge (note that a large fraction of the HA surface layer is still charged at pH 4, based on a pKa of ~ 4) is also advantageous for preparation of more homogeneous, defect free bilayers. Since electrostatic interactions are less likely to interfere with vesicle absorption for the zwitterionic lipids used in the present study, we hypothesize that the lower surface charge is more advantageous for vesicle spreading and rupture.

Bilayers on PEM films have already found a number of applications, for example in creating bilayers on PEM-filled nanopores for biochip development and for delivery of lipophilic cholesterol-based oligonucleotides.^{45,46} The use of biocompatible polysaccharides may be advantageous for these applications. Furthermore, there is scope for modulating the behavior of polysaccharide PEMs by functionalization. For example, a recent study by Winnik

has shown that phosphorylcholine-modified chitosan forms similar PEM films with HA; however, conversion of a fraction of the primary amino groups to secondary amines by covalent attachment of PC groups results in multilayers with higher water content that behave as soft, fluid gels as compared to the hard gels of HA/CHI films.³¹

Finally, it is worth considering the role of surface roughness in formation of supported lipid bilayers. Several studies have concluded that surface roughness is not a major factor in controlling the formation of supported bilayers.^{9,35} For example, bilayers formed by vesicle fusion on silica xerogels follow the surface curvature and have diffusion coefficients that are only a factor of two lower than those on mica, consistent with continuous defect-free bilayers.⁴⁷ It has been argued that most of the decrease in *D* is due to the roughness of the surface, which cannot be easily corrected when determining the diameter of the bleached spot. Similarly, a study of bilayer formation on nanoparticles adsorbed on a mica surface demonstrated that bilayers enveloped and closely followed the particle structure for particles larger than 22 nm in diameter.⁴⁸ However smaller particles (1.2 -22 nm) were located in pores in the membrane. Other studies have shown that the rate and mechanism of bilayer formation via vesicle fusion can be modulated by the use of nanocorrugated vs nanosmooth topographies, with faster vesicle adsorption on the nanocorrugated regions⁴⁹ and that membranes can readily bend to accommodate complex topographies.⁵⁰ The results presented here indicate that surface properties (charge, hydrophilicity) are considerably more important in facilitating vesicle adsorption, spreading and rupture to form bilayers and also in allowing sufficient lipid mobility to form a continuous bilayer with few surface defects.

CONCLUSIONS

Supported lipid bilayers were formed on polysaccharide multilayers produced by sequential adsorption of five CHI/HA bilayers with a top negatively-charged layer to mimic the behavior of glass and mica substrates. At approximately neutral pH, the adsorbed lipids were immobile but a combination of AFM and fluorescence microscopy indicated that this was attributable to formation of a lipid membrane with a combination of defects and pinned lipids, rather than to a layer of unruptured vesicles. At pH 4, supported lipid bilayers with mobile lipids were obtained, and diffusion coefficients measured by FRAP were very similar to those on PEG polymer cushions and approximately a factor of two slower than those on glass. The

formation of mobile lipid bilayers for zwitterionic lipids is in contrast to earlier results indicating that a mixture of charged and zwitterionic lipids was necessary for formation of mobile bilayers on PSS/PAH PEMS with a positively charged top layer.²¹ The ability to generate zwitterionic bilayers on biocompatible polysaccharide films extends the range of utility of PEMS as possible substrates for supported membranes for biosensing applications. Furthermore, the results provide further insight on the relative importance of surface charge and roughness in modulating lipid bilayer formation. Although surface roughness is less important than electrostatic interactions between lipids and the polysaccharide in regulating bilayer formation, it may be responsible for the complex diffusion behavior observed for supported bilayers on PEMS.

ACKNOWLEDGMENT

Partial support of this work from the Natural Sciences and Engineering Research Council is gratefully acknowledged. We thank Z. Lu and M. Chen for imaging support and R. Chisholm for assistance with FRAP data analysis.

References

- (1) Castellana, E. T.; Cremer, P. S. *Surf. Sci. Rep.* **2006**, *61*, 429.
- (2) Chan, Y.-H. M.; Boxer, S. G. *Curr. Opin. Chem. Biol.* **2007**, *11*, 581.
- (3) Sackmann, E. *Science* **1996**, *271*, 43.
- (4) Hughes, A. V.; Howse, J. R.; Dabkowska, A.; Jones, R. A. L.; Lawrence, M. J.; Roser, S. J. *Langmuir* **2008**, *24*, 1989.
- (5) Vockenroth, I. K.; Atansova, P. P.; Long, J. R.; Jenkins, A. T. A.; Knoll, W.; Koper, I. *Biochim. Biophys. Acta* **2007**, *1768*, 1114.
- (6) Kycia, A. H.; Wang, J.; Merrill, A. R.; Lipkowski, J. *Langmuir* **2011**, *27*, ASAP.
- (7) Tanaka, M.; Sackmann, E. *Nature* **2005**, *437*, 656.
- (8) Tanaka, M.; Tutus, M.; Kaufmann, S.; Rossetti, F. F.; Schneck, E.; Weiss, I. M. *J. Struct. Biol.* **2009**, *168*, 137.
- (9) Renner, L.; Osaki, T.; Chiantia, S.; P. Schwille; Pompe, T.; Werner, C. *J. Phys. Chem. B* **2008**, *112*, 6373.
- (10) Tutus, M.; Rosetti, F. F.; Schneck, E.; Fragneto, G.; Forster, F.; Richter, R.; Nawroth, T.; Tanaka, M. *Macromol. Biosci.* **2008**, *8*, 1034.
- (11) Kiessling, V.; Crane, J. M.; Tamm, L. K. *Biophys. J.* **2006**, *91*, 3313.
- (12) Wagner, M. L.; Tamm, L. K. *Biophys. J.* **2000**, *79*, 1400.
- (13) Garg, S.; Ruhe, J.; Ludtke, K.; Jordan, R.; Naumann, C. A. *Biophys. J.* **2007**, *92*, 1263.
- (14) Lin, J.; Szymanski, J.; Searson, P. C.; Hristova, K. *Langmuir* **2010**, *26*, 3544.
- (15) Merzlyakov, M.; Li, E.; Gitsov, I.; Hristova, K. *Langmuir* **2006**, *22*, 10145.
- (16) Deverall, M. A.; Gindl, E.; Sinner, E.-K.; Besir, H.; Ruehe, J.; Saxton, M. J.; Naumann, C. A. *Biophys. J.* **2005**, *88*, 1875.
- (17) Decher, G. *Science* **1997**, *277*, 1232.
- (18) Picart, C.; Mutterer, J.; Richert, L.; Luo, Y.; Prestwich, G. D.; Schaaf, P.; Voegel, J.-C.; Lavalle, P. *Proc. Natl. Acad. Sci.* **2002**, *99*, 12531.
- (19) Bunge, A.; Fischlechner, M.; Loew, M.; Arbuzova, A.; Herrmann, A.; Huster, D. *Soft Matter* **2009**, *5*, 3331.
- (20) Delajon, C.; Gutberlet, T.; Steitz, R.; Mohwald, H.; Krastev, R. *Langmuir* **2005**, *21*, 8509.

- (21) Fischlechner, M.; Zaulig, M.; Meyer, S.; Estrela-Lopis, I.; Cuellar, L.; Irigoyen, J.; Pescador, P.; Brumen, M.; Messner, P.; Moya, S.; Donath, E. *Soft Matter* **2008**, *4*, 2245.
- (22) Kujawa, P.; Moraille, P.; Sanchez, J.; Badia, A.; Winnik, F. M. *J. Am. Chem. Soc.* **2005**, *127*, 9224.
- (23) Richert, L.; Lavalle, P.; Payan, E.; Shu, X. Z.; Prestwich, G. D.; Stoltz, J.-F.; Schaaf, P.; Voegel, J.-C.; Picart, C. *Langmuir* **2004**, *20*, 448.
- (24) Bunge, A.; Loew, M.; Pescador, P.; Arbuzova, A.; Brodersen, N.; Kang, J.; Dahne, L.; Liebscher, J.; Herrmann, A.; Stengel, G.; Huster, D. *J. Phys. Chem. B* **2009**, *113*, 16425.
- (25) Croll, T. I.; O'Connor, A. J.; Stevens, G. W.; Cooper-White, J. J. *Biomacromolecules* **2006**, *7*, 1610.
- (26) Mansouri, S.; Fatisson, J.; Miao, Z.; Merhi, Y.; Winnik, F. M.; Tabrizian, M. *Langmuir* **2009**, *25*, 14071.
- (27) Pavinatto, F. J.; Caseli, L.; Oliviera, O. N. *Biomacromolecules* **2010**, *11*, 1897.
- (28) Gerelli, Y.; Di Bari, M. T.; Deriu, A.; Clemens, D.; Almasy, L. *Soft Matter* **2010**, *6*, 2533.
- (29) Lapcik, L., Jr.; Lapcik, L.; De Smedt, S.; Demeester, J.; Chabreck, P. *Chem. Rev.* **1998**, *98*, 2663.
- (30) Kumar, M. N. V. R.; Muzzarelli, R. A. A.; Muzzarelli, C.; Sashiwa, H.; Domb, A. J. *Chem. Rev.* **2004**, *104*, 6017.
- (31) Kujawa, P.; Schmauch, G.; Viitala, T.; Badia, A.; Winnik, F. M. *Biomacromolecules* **2007**, *8*, 3169.
- (32) Soumpasis, D. M. *Biophys. J.* **1983**, *41*, 95.
- (33) Kujawa, P.; Sanchez, J.; Badia, A.; Winnik, F. M. *J. Nanosci. Nanotechnol.* **2006**, *6*, 1565.
- (34) Salomaki, M.; Kankare, J. *Biomacromolecules* **2009**, *10*, 294.
- (35) Richter, R. P.; Berat, R.; Brisson, A. R. *Langmuir* **2006**, *22*, 3497.
- (36) Machan, R.; Hof, M. *Biochim. Biophys. Acta* **2010**, *1798*, 1377.
- (37) Seu, K. J.; Pandey, A. P.; Haque, F.; Proctor, E. A.; Ribbe, A. E.; Hovis, J. S. *Biophys. J.* **2007**, *92*, 2445.
- (38) Bayerl, T. M.; Bloom, M. *Biophys. J.* **1990**, *58*, 357.
- (39) Lin, W.-C.; Blanchette, C. D.; Ratto, T. V.; Longo, M. L. *Biophys. J.* **2006**, *90*, 228.

- (40) Cha, T.; Guo, A.; Zhu, X.-Y. *Biophys. J.* **2006**, *80*, 1270.
- (41) Ira; Zou, S.; Carter Ramirez, D. M.; Vanderlip, S.; Ogilvie, W.; Jakubek, Z.; Johnston, L. J. *J. Struct. Biol.* **2009**, *168*, 78.
- (42) Johnston, L. J. *Langmuir* **2007**, *23*, 5886.
- (43) Merzlyakov, M.; Li, E.; Hristova, K. *Langmuir* **2006**, *22*, 1247.
- (44) Kaufmann, S.; Papastavrou, G.; Kumar, K.; Textor, M.; Reimhult, E. *Soft Matter* **2009**, *5*, 2804.
- (45) Sugihara, K.; Vanos, J.; Zambelli, T. *ACS Nano* **2010**, *4*, 5047.
- (46) Bunge, A.; Loew, M.; Pescador, P.; Arbuzova, A.; Brodersen, N.; Kang, J.; Dahne, L.; Liebscher, J.; Herrmann, A.; Stengel, G.; Huster, D. *J. Phys. Chem. B* **2009**, *113*, 16425.
- (47) Goksu, E. I.; Hoopes, M. I.; Nellis, B. A.; Xing, C.; Faller, R.; Frank, C. W.; Risbud, S. H.; Satcher, J. H.; Longo, M. L. *Biochim. Biophys. Acta* **2010**, *1798*, 719.
- (48) Roiter, Y.; Ornatska, M.; Rammohan, A. R.; Balakrishnan, J.; Heine, D. R.; Minko, S. *Langmuir* **2009**, *25*, 6287.
- (49) Lee, S.-W.; Na, Y.-J.; Lee, S.-D. *Langmuir* **2009**, *25*, 5421.
- (50) Sanii, B.; Smith, A. M.; Butti, R.; Brozell, A. M.; Parikh, A. N. *Nano Lett.* **2008**, *8*, 866.

Table 1. Surface thickness and RMS roughness measured by AFM for CHI/HA films on various supports.

<u>PEM – support</u>	<u>pH</u>	<u>thickness, nm</u>	<u>rms, nm</u>
(CHI/HA) ₅ – glass	6.5	57±3	25±2
(CHI/HA) ₅ – glass	4.0	31±4	15±3
PEI/HA/(CHI/HA) ₅ – glass	6.5	54±4	25±3
(CHI/HA) ₅ – silicon	6.5	52±5	23±2

Table 2. Diffusion coefficients, D, and mobile lipid fractions, F, obtained by FRAP measurements for OG-DHPE in DOPC bilayers on various supports.

<u>Support</u>	<u>pH</u>	<u>D, $\mu\text{m}^2/\text{s}$</u>	<u>F, %</u>
Glass	6.5	4.4 ± 0.3	>99
(CHI/HA) ₅	6.5	0.3 ± 0.3	22 ± 15
(CHI/HA) ₅	7.0 [#]	2.8 ± 0.2	>99
(CHI/HA) ₅	4.0	2.49 ± 0.07	>99
PEG	4.5	2.16 ± 0.07	>99

[#] Bilayer prepared at pH 4 and then washed with pH 7 buffer prior to FRAP experiment.

Figure Captions

Figure 1. AFM images of (CHI/HA)₅ polymer films on a glass substrate imaged in water at pH 6.5. Images B and C show samples before and after scratching away part of the polymer film. Image D is for (CHI/HA)₅ on silicon.

Figure 2. Fluorescence images of membranes obtained by incubating DOPC vesicles containing 0.2 mol% Texas Red-DHPE (A,B) or OG-DHPE (C) on a (CHI/HA)₅ polymer film (A, C) on a glass substrate and on glass (B). Samples were prepared by incubation at pH 6.5.

Figure 3. FRAP experiment for a membrane obtained by incubating DOPC vesicles containing 0.2 mol% Oregon Green-DHPE on a (CHI/HA)₅ polymer film on glass: A, before bleaching; B, immediately after bleaching; C, D, E at 118, 183 and 1330 s after bleaching. F shows a plot of fluorescence intensity as a function of time, demonstrating a large immobile lipid fraction.

Figure 4. AFM images of a membrane prepared by incubating DOPC vesicles on a (CHI/HA)₅ polymer film on glass at pH 6.5: A, height; B, deflection.

Figure 5. Fluorescence images of bilayers obtained by incubating DOPC vesicles on a (CHI/HA)₅ polymer film on glass (A, Texas Red-DHPE; B, Oregon Green-DHPE) at pH 4. (C, D) Fluorescence images obtained at higher magnification (150x) for DOPC (C) and DOPC/egg sphingomyelin/cholesterol (D) vesicles incubated on (CHI/HA)₅ polymer films.

Figure 6. FRAP experiment for a DOPC bilayer on a (CHI/HA)₅ polymer film. Images were recorded before (A), immediately after (B) and 11, 45 and 750 (C, D, E) seconds after photobleaching, respectively. (F) The corresponding FRAP recovery curve, with $D = 2.5 \mu\text{m}^2/\text{s}$.

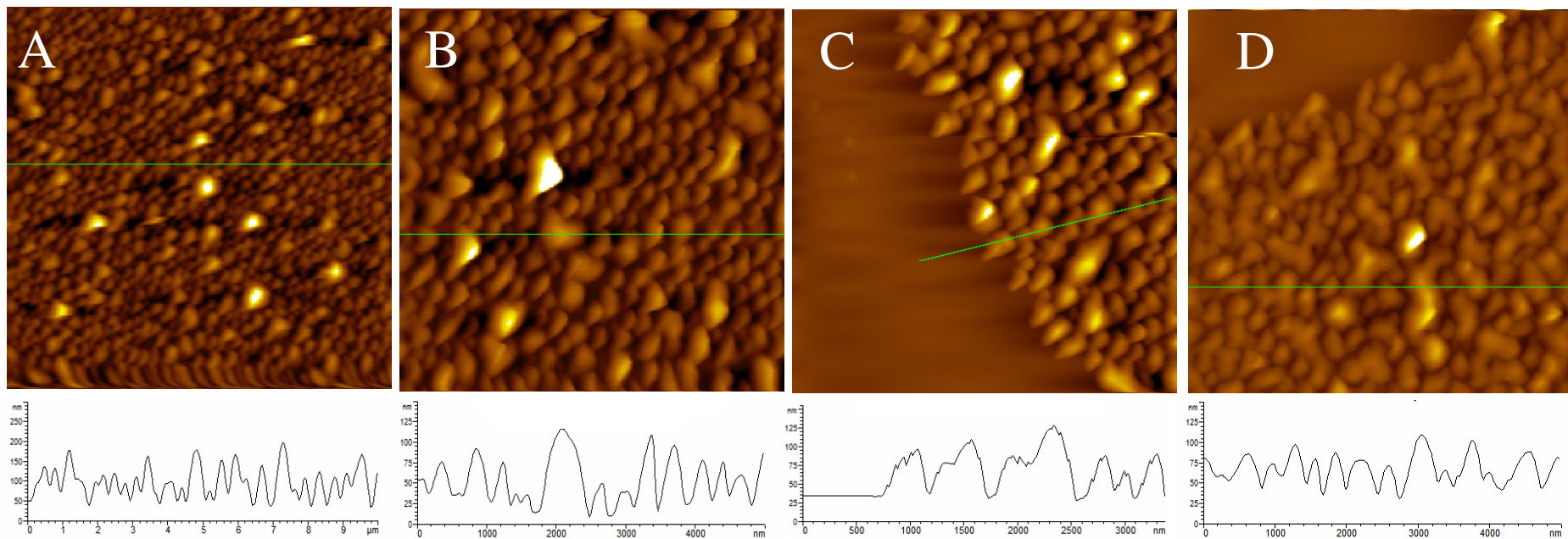


Figure 1. AFM images of $(\text{CHI}/\text{HA})_5$ polymer films on a glass substrate imaged in water at pH 6.5. Images B and C show samples before and after scratching away part of the polymer film. Image D is for $(\text{CHI}/\text{HA})_5$ on silicon.

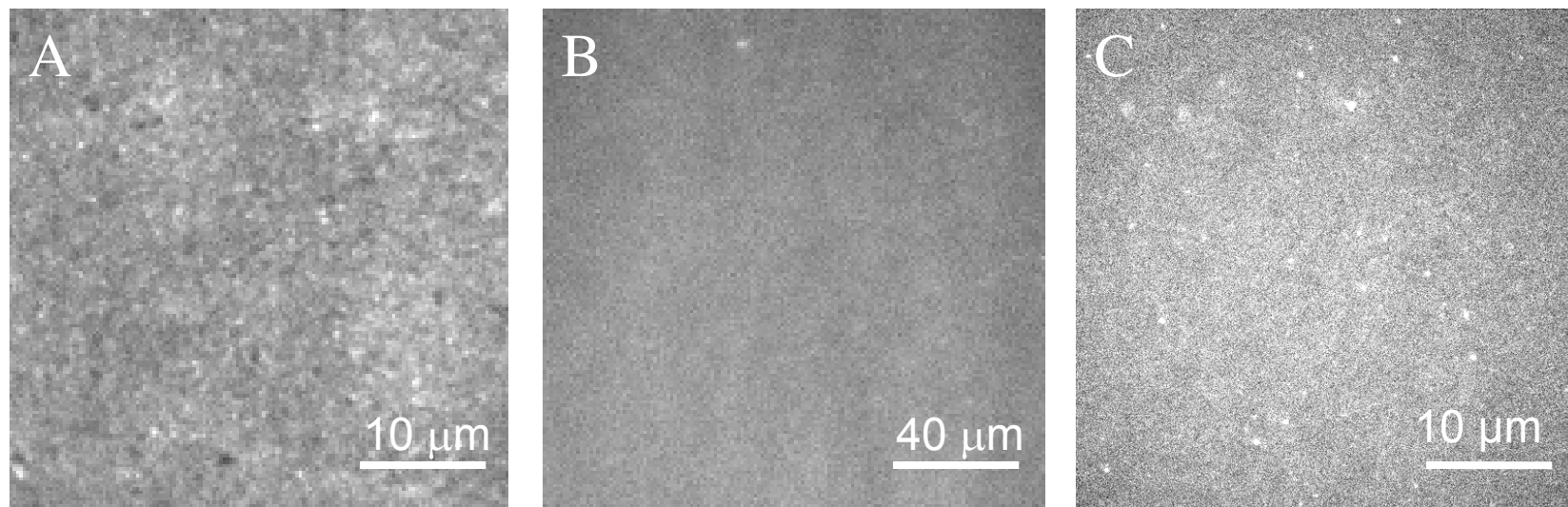


Figure 2. Fluorescence images of membranes obtained by incubating DOPC vesicles containing 0.2 mol% Texas Red-DHPE (A,B) or OG-DHPE (C) on a (CHI/HA)₅ polymer film (A, C) on a glass substrate and on glass (B). Samples were prepared by incubation at pH 6.5.

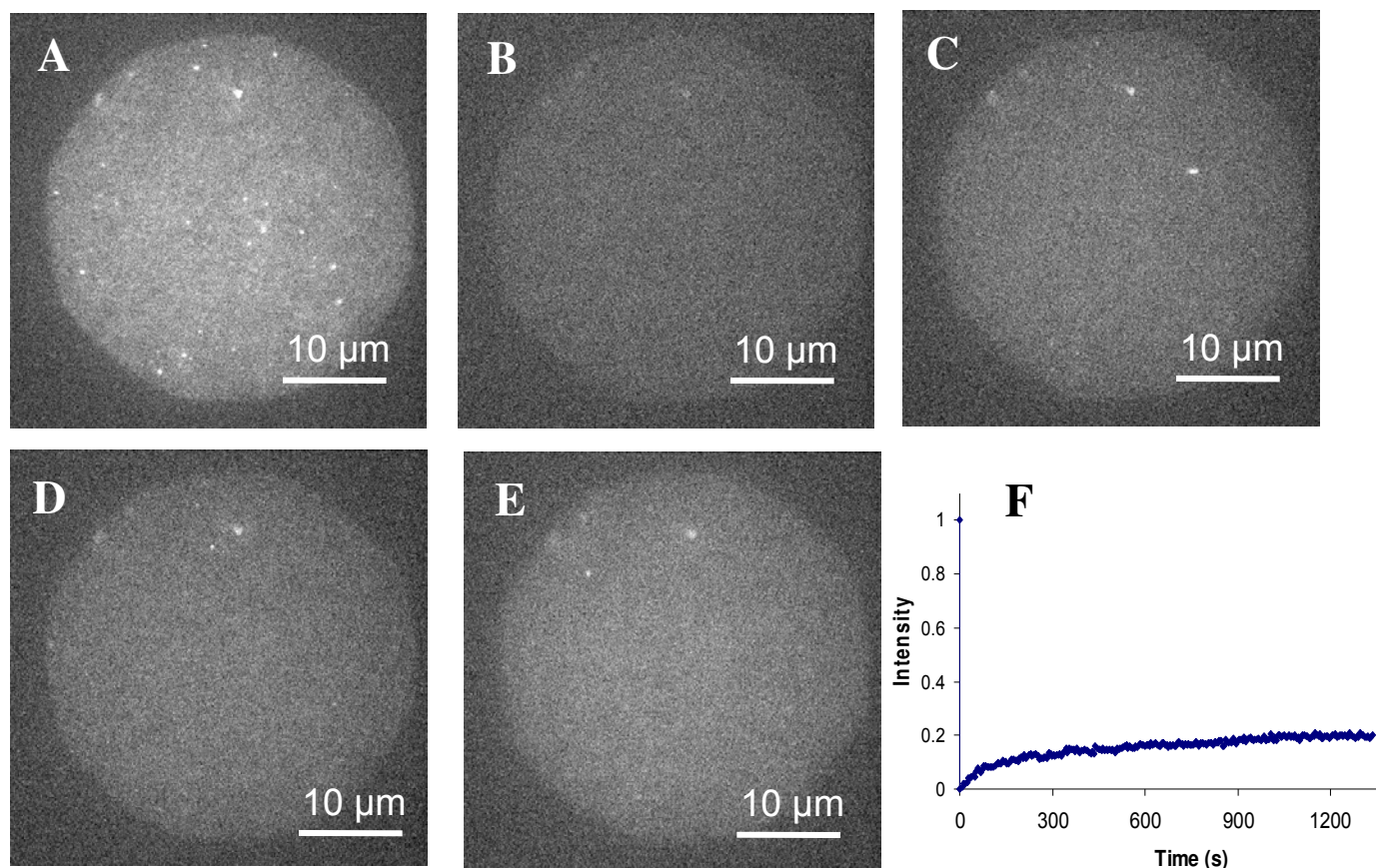


Figure 3. FRAP experiment for a membrane obtained by incubating DOPC vesicles containing 0.2 mol% Oregon Green-DHPE on a (CHI/HA)₅ polymer film on glass: A, before bleaching; B, immediately after bleaching; C, D, E at 118, 183 and 1330 s after bleaching. F shows a plot of fluorescence intensity as a function of time, demonstrating a large immobile lipid fraction.

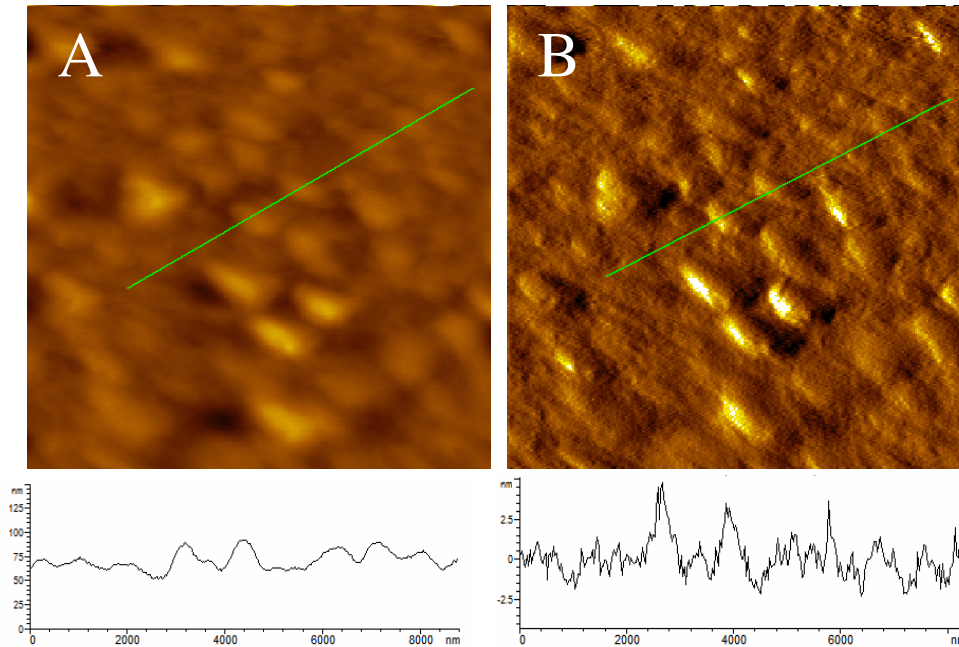


Figure 4. AFM images of a membrane prepared by incubating DOPC vesicles on a (CHI/HA)₅ polymer film on glass at pH 6.5: A, height; B, deflection.

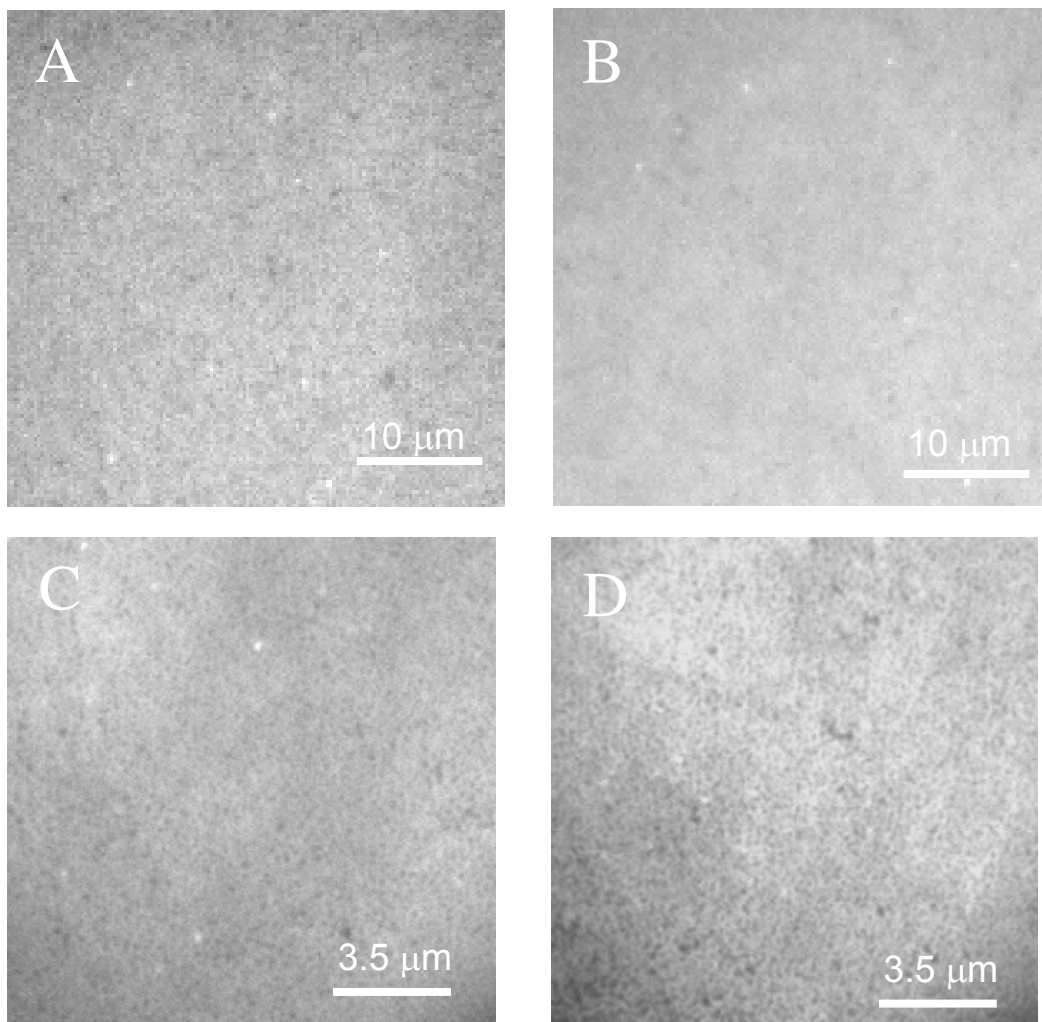


Figure 5. Fluorescence images of bilayers obtained by incubating DOPC vesicles on a $(\text{CHI}/\text{HA})_5$ polymer film on glass (A, Texas Red-DHPE; B, Oregon Green-DHPE) at pH 4. (C,D) Fluorescence images obtained at higher magnification (150x) for DOPC (C) and DOPC/egg sphingomyelin/cholesterol (D) vesicles incubated on $(\text{CHI}/\text{HA})_5$ polymer films.

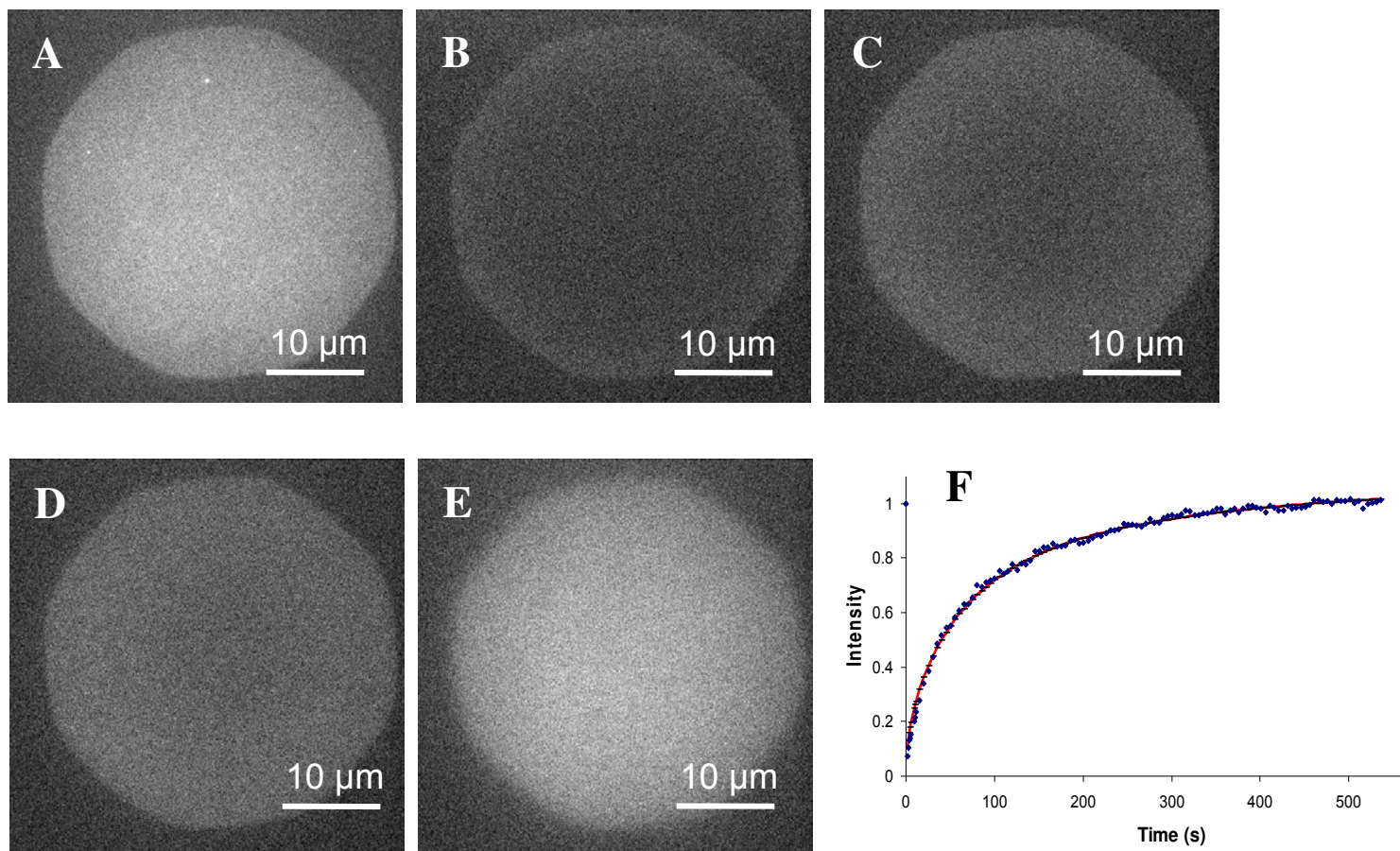


Figure 6. FRAP experiment for a DOPC bilayer on a $(\text{CHI/HA})_5$ polymer film. Images were recorded before (A), immediately after (B) and 11, 45 and 750 (C, D, E) seconds after photobleaching, respectively. (F) The corresponding FRAP recovery curve, with $D = 2.5 \mu\text{m}^2/\text{s}$.